Nanocatalysis

DOI: 10.1002/anie.201406463

Insights into the Catalytic Activity of Nitridated Fibrous Silica (KCC-1) Nanocatalysts from ^{15}N and ^{29}Si NMR Spectroscopy Enhanced by Dynamic Nuclear Polarization**

Aany Sofia Lilly Thankamony, Cédric Lion, Frédérique Pourpoint, Baljeet Singh, Angel J. Perez Linde, Diego Carnevale, Geoffrey Bodenhausen, Hervé Vezin, Olivier Lafon, and Vivek Polshettiwar**

Abstract: *Fibrous nanosilica (KCC-1) oxynitrides are promising solid-base catalysts. Paradoxically, when their nitrogen content increases, their catalytic activity decreases. This counterintuitive observation is explained here for the first time using ^{15}N-solid-state NMR spectroscopy enhanced by dynamic nuclear polarization.*

High surface area silica materials have applications in many fields, including catalysis, medical imaging, and drug delivery.[1] Nevertheless, poor accessibility to active sites can limit applications where mass transport is vital. Hence, higher surface silica nanospheres with better accessibility are needed. Recently, we discovered KCC-1 silica nanospheres,[2] and observed that their unique fibrous morphology dramatically increases accessibility of active sites.[2–7] However, KCC-1 is made of neutral silica frameworks, without active sites, thus limiting its application to fields like adsorption and catalysis. To overcome this limitation, we explored the functionalization and metal coating of KCC-1 for supported catalytic systems.[3–5]

Recently, KCC-1 silicon oxynitride was prepared by ammonolysis and showed excellent activity for CO_2 capture[6] and as a solid base.[7] Higher nitridation temperatures (T_N) increase the nitrogen content of these silicon oxynitrides, but, paradoxically, decrease their catalytic activity. This property has not been explained so far, despite exhaustive characterization by N_2 sorption, TEM, SEM, XPS, FT-IR, etc. Similarly, previous studies by conventional NMR techniques did not allow the identification of the silylamine sites in nitridated mesoporous silica.[7–11]

Herein, we explain for the first time the decrease of the catalytic activity of nitridated KCC-1 when increasing the nitrogen content. This phenomenon is due to the conversion of primary silylamine sites into secondary ones at T_N values greater than or equal to 800 °C. This structural information is obtained by solid-state ^{15}N NMR spectrosocpy, where the sensitivity is boosted by dynamic nuclear polarization (DNP). DNP-enhanced ^{29}Si NMR spectra also prove the formation of geminal amine surface sites (separated by two Si–N bonds) at T_N values greater than or equal to 800 °C. This work is the first application of DNP-enhanced NMR spectroscopy to moisture-sensitive fibrous nanoparticles. So far, DNP NMR spectroscopy has been demonstrated for nonporous or mesoporous nanoparticles.[12–16]

Nitridation of KCC-1 was performed by treating KCC-1 with pure ammonia (300 mL min^{-1}) at various nitridation temperatures, T_N, for 12 hours (see the Supporting Information). The samples are labeled by KCC-1-NT_N to indicate the nitridation temperature. Samples named KCC-1-^{15}NT_N are enriched in ^{15}N. As shown in Table 1, the nitrogen content increases with T_N. For KCC-1-^{15}N1100, the N content was lower than that for KCC-1-N900, because of a shorter reaction time (3 h) and reduced ammonia flow (50 mL min^{-1}). We did not observe any significant changes in shape, size, and morphology after nitridation at various T_N values (see Figure 1).

[*] Dr. A. S. Lilly Thankamony, Dr. F. Pourpoint, Prof. O. Lafon
Univ. Lille Nord de France, Unite de Catalyse et de Chimie du Solide (UCCS), CNRS UMR 8181
Univ. Lille 1, 59652 Villeneuve d'Ascq (France)
E-mail: olivier.lafon@univ-lille1.fr
Dr. C. Lion
Univ. Lille Nord de France, Unité de Glycobiologie Structurale et Fonctionnelle (UGSF), CNRS UMR 8576
Univ. Lille 1, 59652 Villeneuve d'Ascq (France)
B. Singh, Prof. V. Polshettiwar
Nanocatalysis Laboratory (NanoCat), Division of Chemical-Sciences, Tata Institute of Fundamental Research (TIFR)
Mumbai (India)
E-mail: vivekpol@tifr.res.in
Dr. A. J. Perez Linde, Dr. D. Carnevale, Prof. G. Bodenhausen
Institut des Sciences et Ingénierie Chimiques
Ecole Polytechnique Fédérale de Lausanne (EPFL)
1015 Lausanne (Switzerland)
Dr. H. Vezin
Univ. Lille Nord de France, Laboratoire de Spectrochimie Infrarouge et Raman (LASIR), CNRS UMR 8516
Univ. Lille 1, 59652 Villeneuve d'Ascq (France)

[**] This work was supported by the Region Nord/Pas de Calais, the European Union (FEDER), the CNRS, the French ministry of research, USTL, ENSCL, contracts ANR-2020-jcjc-0811-01, CEFIPRA n°5208-E, COST TD 1103, the Swiss National Science Foundation, the Swiss Commission for Technology and Innovation, the EPFL, and Bruker Biospin. V.P. thanks the Department of Atomic Energy (DAE), Government of India for a start-up grant at Tata Institute of Fundamental Research (TIFR), Mumbai.

Supporting information for this article is available on the WWW under http://dx.doi.org/10.1002/anie.201406463.

Table 1: Textural properties and nitrogen content of nitridated KCC-1.

Sample	BET surface area [$m^2 g^{-1}$]	Langmuir surface area [$m^2 g^{-1}$]	BJH pore volume [$cm^3 g^{-1}$]	Nitrogen content[a] [wt%]
KCC-1	669	964	1.27	0
KCC-1-N600	603	871	1.22	2.02
KCC-1-^{15}N700	610	885	1.29	3.18
KCC-1-N800	565	815	1.17	6.37
KCC-1-N900	492	711	1.06	11.94
KCC-1-^{15}N1100	285	399	0.72	6.52

[a] Determined by C,H,N analysis.

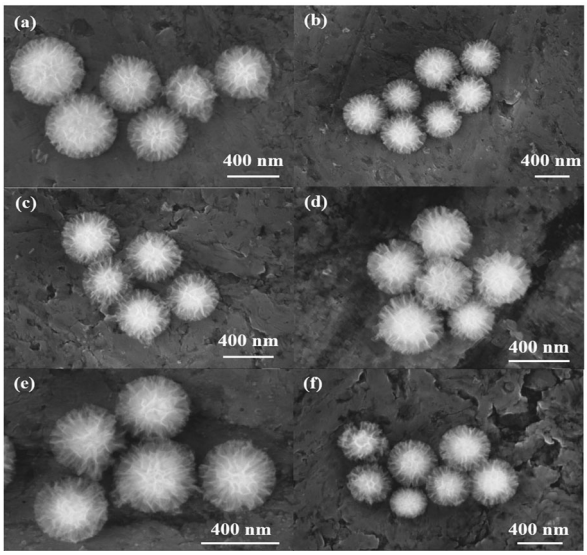

Figure 1. SEM images of a) KCC-1, b) KCC-1-N600, c) KCC-1-N700, d) KCC-1-N800, e) KCC-1-N900, and f) KCC-1-N1100.

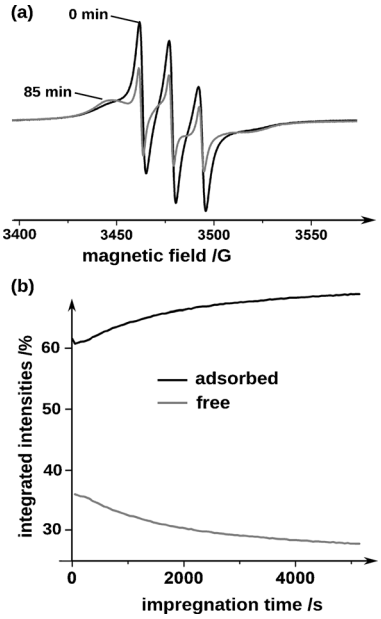

Figure 2. a) X-band EPR spectra of a KCC-1-N900 sample impregnated with a 16 mM bTbK solution in TCE at 298 K after an impregnation time of 0 (black) and 85 min (gray). b) Evolution of the doubly integrated EPR signals corresponding to free (gray) and adsorbed (black) bTbK molecules as a function of the impregnation time.

For DNP NMR experiments, KCC-1-N samples were impregnated with a solution of bis(TEMPO)-bis(ketal) (bTbK) biradical (TEMPO = 2,2,6,6-tetramethylpiperidin-1-oxyl) in 1,1,2,2-tetrachloroethane (TCE).[17] TCE was used since nitridated KCC-1 is moisture sensitive.[18] Here, bTbK was synthesized in two steps with a 51% overall yield, according to a procedure adapted from the literature with slight modifications.[17] The bTbK was obtained by oxidation of diamine precursor using sodium tungstate dihydrate in 30% aqueous hydrogen peroxide and methanol (see the Supporting Information).

The EPR spectrum of KCC-1-N900 right after impregnation with 16 mM bTbK solution was dominated by a narrow triplet corresponding to bTbK molecules in solution. A broader and less intense triplet with a larger splitting was also visible. This broadening can be ascribed to the anisotropic hyperfine coupling with ^{14}N in bTbK molecules adsorbed onto the KCC-1-N900 surface. The deconvolution of the EPR spectrum shows that the fraction of adsorbed bTbK molecules was larger than that of free bTbK. During impregnation, the fraction of adsorbed bTbK increases (see Figure 2b).

Figure 3a shows how the sensitivity enhancement afforded by DNP permits the detection of ^{1}H→^{15}N cross-polarization magic-angle spinning (CPMAS) spectra of KCC-1-N900 with ^{15}N in natural abundance (0.37%), whereas these signals can hardly be detected without microwave irradiation. The enhancement factor per scan resulting from microwave irradiation was $\varepsilon^{scan}_{on/off} > 17$. For ^{15}N-enriched samples, the enhancement factor was $\varepsilon^{scan}_{on/off} \approx 30$ (see Figure S7 in the Supporting Information). As expected, a similar enhancement was observed for the ^{1}H polarization (see Figure S8). Furthermore, as for other biradicals, the build-up time, $T_{DNP}(^1H)$, of the ^{1}H magnetization enhanced by DNP was found to be equal to the longitudinal relaxation time, $T_{DNP}(^1H) = T_1(^1H) = 8.5$ s. Hence, for KCC-1-N900, it would take more than 900 days (see the Supporting Information) to obtain a ^{1}H→^{15}N CPMAS spectrum without microwave irradiation, with a similar S/N ratio as that in Figure 3a.

The ^{1}H→^{15}N CPMAS preferentially enhances the polarization of ^{15}N nuclei near the surface, since there are few protons in the bulk of silicon oxynitrides. The comparison of DNP-enhanced ^{1}H→^{15}N CPMAS spectra in Figures 3b–f show that the local environments of the ^{15}N nuclei are affected by T_N. The ^{15}N spectra of KCC-1-N600 and KCC-1-^{15}N700 are dominated by two resolved peaks near $\delta = 10$ and 25 ppm and can be assigned to NH_2Si and $NHSi_2$ sites, respectively.[19,20] The deconvolution of the KCC-1-^{15}N700 spectrum indicates the presence of an additional site near $\delta =$ 0 ppm, which can be assigned to ammonium ions.[21] In none of the samples could we detect any signals for $^{15}NH_3$ near $\delta =$ −32 ppm.[22] For T_N values greater than or equal to 800 °C, the $NHSi_2$ peak becomes dominant. Its chemical shift increases with increasing T_N. This increase must stem from the formation of geminal amine sites, as evidenced by ^{29}Si NMR spectroscopy. Furthermore, the spectra of KCC-N900 and

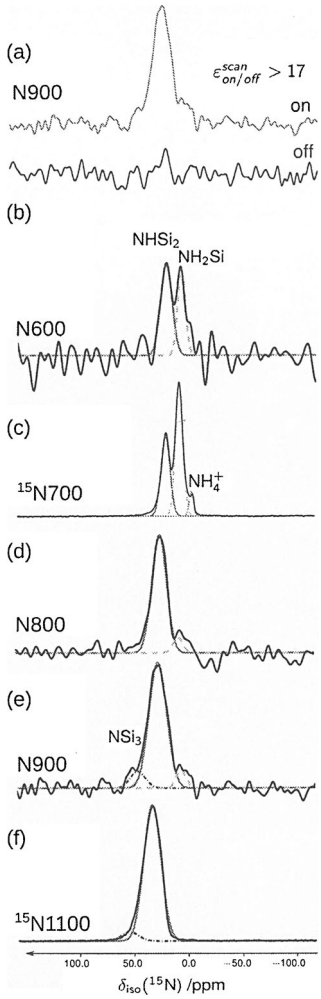

Figure 3. a) $^{1}H \rightarrow {}^{15}N$ CPMAS spectra obtained of KCC-1-N900 impregnated with a 16 mM bTbK solution in TCE at 100 K, 9.4 T and $\nu_r = 8$ kHz with (gray) and without (black) microwave irradiation. DNP-enhanced $^{1}H \rightarrow {}^{15}N$ CPMAS spectra of b) KCC-1-N600, c) KCC-1-^{15}N700, d) KCC-1-N800, e) KCC-1-N900, and f) KCC-1-^{15}N1100 under the same conditions. The components of the best-fit simulations are represented by dot-dash (NSi_3), continuous gray ($NHSi_2$), dashed (NH_2Si), and dotted (NH_4^+) lines using the parameters given in Table S1.

KCC-^{15}N1100 display a signal of NSi_3 sites at $\delta = 55$ ppm.[23] Figures 3 b–f shows that the surface nitrogen atoms are bonded to an increasing number of silicon atoms when increasing T_N. This NMR observation is in agreement with earlier XPS studies.[7]

These DNP NMR results indicate that for T_N values less than or equal to 700 °C, the surface nitrogen sites of KCC-1-N correspond to primary (NH_2Si) and secondary ($NHSi_2$) amines. From a T_N value of 700 to 1100 °C, the concentration of $SiNH_2$ decreases, whereas that of $NHSi_2$ increases. These observations clearly agree with the catalytic activity of these materials[7] since NH_2Si is catalytically more active than $NHSi_2$ and KCC-1-N prepared at $500 \leq T_N \leq 700$ °C achieves the highest conversion for Knoevenagel condensation reactions. Thus our DNP-enhanced ^{15}N NMR study provides for the first time an understanding of the reduced catalytic activity of KCC-1-N with increasing nitrogen contents.

DNP at 9.4 T can also boost the sensitivity of $^{1}H \rightarrow {}^{29}Si$ CPMAS experiments.[14] DNP-enhanced $^{1}H \rightarrow {}^{29}Si$ CPMAS spectra, shown in Figure S10, indicate that the surface Si sites are bound to a larger number of N atoms at higher T_N values. The lower fraction of Q^3 sites with respect to Q^4 sites with increasing T_N values (see Table S2) proves that silanol groups are more reactive toward NH_3 than siloxane bridges in KCC-1.

Based on the ^{15}N and ^{29}Si DNP NMR spectra and the previously reported mechanisms for the nitridation of MCM-41,[10] we propose a mechanism for the KCC-1 nitridation. This mechanism involves the attack of NH_3 on 1) silanol groups to form primary silylamine (see Scheme S3) or on 2) the siloxane bridge to form primary amines and subsequently secondary and tertiary amines (see Scheme S4).

In conclusion, we have shown for the first time that the decrease in the catalytic activity of KCC-1-N prepared at higher T_N values stems from the disappearance of primary amine sites and the formation of secondary ones. This novel structural information has been derived from solid-state ^{15}N DNP NMR spectroscopy. Furthermore, the EPR spectra provided direct evidence for the adsorption of bTbK onto the KCC-1-N surface.

Received: June 22, 2014
Revised: August 27, 2014
Published online: December 2, 2014

Keywords: EPR spectroscopy · nanostructures · NMR spectroscopy · fibrous silica (KCC-1) · nanocatalysis

[1] B. Lebeau, A. Galarneau, M. Linden, *Chem. Soc. Rev.* **2013**, *42*, 3661 – 3662 and references therein.
[2] V. Polshettiwar, D. Cha, X. Zhang, J. M. Basset, *Angew. Chem. Int. Ed.* **2010**, *49*, 9652 – 9656; *Angew. Chem.* **2010**, *122*, 9846 – 9850.
[3] V. Polshettiwar, J. Thivolle-Cazat, M. Taoufik, F. Stoffelbach, S. Norsic, J.-M. Basset, *Angew. Chem. Int. Ed.* **2011**, *50*, 2747 – 2751; *Angew. Chem.* **2011**, *123*, 2799 – 2803.
[4] A. Fihri, D. Cha, M. Bouhrara, N. Almana, V. Polshettiwar, *ChemSusChem* **2012**, *5*, 85 – 89.
[5] A. Fihri, M. Bouhrara, U. Patil, D. Cha, Y. Saih, V. Polshettiwar, *ACS Catal.* **2012**, *2*, 1425 – 1431.
[6] U. Patil, A. Fihri, A.-H. Emwas, V. Polshettiwar, *Chem. Sci.* **2012**, *3*, 2224 – 2229.
[7] M. Bouhrara, C. Ranga, A. Fihri, R. R. Shaikh, P. Sarawade, A.-H. Emwas, M. N. Hedhili, V. Polshettiwar, *ACS Sustainable Chem. Eng.* **2013**, *1*, 1192 – 1199.
[8] A. Bendjeriou-Sedjerari, J. D. A. Pelletier, E. Abou-Hamad, L. Emsley, J.-M. Basset, *Chem. Commun.* **2012**, *48*, 3067 – 3069.
[9] J. El Haskouri, S. Cabrera, F. Sapiña, J. Latorre, C. Guillem, A. Beltrán-Porter, D. Beltrán-Porter, M. D. Marcos, P. Amorós, *Adv. Mater.* **2001**, *13*, 192 – 195.
[10] T. Asefa, M. Kruk, N. Coombs, H. Grondey, M. J. MacLachlan, M. Jaroniec, G. A. Ozin, *J. Am. Chem. Soc.* **2003**, *125*, 11662 – 11673.
[11] F. Hayashi, K. Ishizu, M. Iwamoto, *J. Am. Ceram. Soc.* **2010**, *93*, 104 – 110.
[12] V. Vitzthum, P. Miéville, D. Carnevale, M. A. Caporini, D. Gajan, C. Copéret, M. Lelli, A. Zagdoun, A. J. Rossini, A.

Lesage, L. Emsley, G. Bodenhausen, *Chem. Commun.* **2012**, *48*, 1988 – 1990.
[13] O. Lafon, A. S. Lilly Thankamony, T. Kobayashi, D. Carnevale, V. Vitzthum, I. I. Slowing, K. Kandel, H. Vezin, J.-P. Amoureux, G. Bodenhausen, M. Pruski, *J. Phys. Chem. C* **2013**, *117*, 1375 – 1382.
[14] T. Kobayashi, O. Lafon, A. S. Lilly Thankamony, I. I. Slowing, K. Kandel, D. Carnevale, V. Vitzthum, H. Vezin, J.-P. Amoureux, G. Bodenhausen, M. Pruski, *Phys. Chem. Chem. Phys.* **2013**, *15*, 5553 – 5562.
[15] O. Lafon, A. S. Lilly Thankamony, M. Rosay, F. Aussenac, X. Lu, J. Trébosc, V. Bout-Roumazeilles, H. Vezin, J.-P. Amoureux, *Chem. Commun.* **2013**, *49*, 2864 – 2866.
[16] Ü. Akbey, B. Altin, A. Linden, S. Özçelik, M. Gradzielski, H. Oschkinat, *Phys. Chem. Chem. Phys.* **2013**, *15*, 20706 – 20716.
[17] Y. Matsuki, T. Maly, O. Ouari, H. Karoui, F. Le Moigne, E. Rizzato, S. Lyubenova, J. Herzfeld, T. Prisner, P. Tordo, R. G. Griffin *Angew. Chem. Int. Ed. Engl.* **2009**, *48*, 4996 – 5000; *Angew. Chem.* **2009**, *121*, 5096 – 5100.
[18] A. Zagdoun, A. J. Rossini, D. Gajan, A. Bourdolle, O. Ouari, M. Rosay, W. E. Maas, P. Tordo, M. Lelli, L. Emsley, A. Lesage, C. Copéret, *Chem. Commun.* **2012**, *48*, 654 – 656.
[19] E. Brendler, S. Frühauf, E. Müller, G. Roewer, *Chem. Mater.* **2004**, *16*, 1368 – 1376.
[20] G. Motz, T. Schmalz, G. Glatz, R. Kempe, W. Milius, B. Wrackmeyer, *Z. Anorg. Allg. Chem.* **2010**, *636*, 1056 – 1060.
[21] J. Mason, "Nitrogen NMR" in *Encyclopedia of Magnetic Resonance* (Eds: R. K. Harris, R. E. Wasylishen), John Wiley, Chichester, DOI: 10.1002/9780470034590.emrstm0343. Posted online 15th March 2007.
[22] G. P. Holland, B. R. Cherry, T. M. Alam, *J. Phys. Chem. B* **2004**, *108*, 16420 – 16426.
[23] E. Leonova, J. Grins, M. Shariatgorji, L. L. Ilag, M. Edén, *Solid State Nucl. Magn. Reson.* **2009**, *36*, 11 – 18.

